Report No. 45

April, 1951.

THE COLLEGE OF AERONAUTICS

CRANFIELD

Tests on the General Instability of a Stiffened Metal Cylinder under Axial Compression

- by -

W.R. Heald, B.E(Mech)(N.Z.), D.C.Ae.

--ooOoo--

SUMMARY

A thin stiffened metal cylinder liable to General Instability was tested under axial compression and an investigation was made into possible methods of predicting the critical load from non-destructive tests. Particular attention was paid to the perturbation loading technique. The cylinder was finally tested to destruction and the actual failing load compared with the values given by various theories and empirical relationships.

It was not possible to predict the critical load from measurements of the normal restraint coefficient (or radial stiffness); the stiffness did not vary with end load according to any simple law, being sensitive to the amount of skin buckling and falling off very rapidly over the last small fraction of the load.

The possibility was indicated of finding the buckled wave form at failure from measurements of the cylinder distortion during comparatively light compression load tests and/or radial perturbation loads.

Very good agreement was obtained between the failing load on test and the values predicted from Hoff's semi-empirical law and van der Neut's theoretical relationship, though in both cases the solution depended on some test information.

YSB

1. Introduction

In the past, frame sizes of stressed skin metal aircraft have been dictated mainly by local loading conditions and manufacturing considerations. Considered solely on the basis of maintaining the cross-sectional shape of the structure and giving it the necessary stiffness, these frames have been unnecessarily heavy. In the interests of weight saving it now becomes possible in the case of very large aircraft to reduce frame sizes to nearer the theoretical minimum.

Past aircraft structural failures have been confined to material failures, local instability and panel instability, but with the relative reduction in frame sizes a further possibility arises, namely General Instability.

A General Instability failure is characterised by the simultaneous collapse at the critical load of all three structural elements, the skin, the stringers, and the frames.

In some earlier tests by H.B. Grant at the College of Aeronautics, it was found that the normal restraint coefficient could not be used to predict the critical load, but the possibility was observed of correlating the final buckled wave form with the deflection pattern under radial perturbation loads.

It was considered that Grant's results may have been unduly affected by end constraints, so for these further tests the original cylinder was almost doubled in length.

2. Description of Test Cylinder, Loading System and Instrumentation.

2.1 The Cylinder

The cylinder used for Grant's earlier tests had failed in General Instability, but on unloading, owing to the semi-elastic nature of the failure, had returned largely to its original form, apart from a small permanent set in a few stringers and some slight skin buckling. To get the required total length for these later tests, Grant's cylinder and a similar unused one were joined together. One end of each cylinder was cut away as far as the first frame and the cylinders were joined by a simple circumferential lap joint of the skins under the centre frame of the resulting cylinder. So as to reduce the effects of this discontinuity to a minimum the thickness of the centre frame was reduced so that, with the extra local thickness of skin, it gave approximately the same moment of inertia as the other frames. New stringers were fitted, continuous from end to end of the cylinder. For ease of assembly and later modifications, all the stringers and frames were attached with 4 BA bolts.

Essentially the cylinder consisted of a thin cylindrical shell (see Figs. 1 and 4) of 22 s.w.g. aluminium alloy sheet (D.T.D.390), 33.5 ins. diameter and 10 ft. 11 ins. length, stiffened by 21 inverted top-hat stringers (see Fig.2) equally spaced around the circumference and 7 flat rectangular frames, 0.5 ins. x 10 s.w.g., at 20 ins. spacing. The ends of the cylinder were stiffened locally with a double skin and riveted between two rings of 1" x 1" x 1/8" angle

/so as ...

so as to distribute the applied compressive loads reasonably uniformly into the cylinder.

Note: Reference System for Points on the Cylinder.

Points on the cylinder are referred to by the frame letter followed by the stringer number. Thus C9 refers to the intersection of Frame 'C' with Stringer '9'; but CD9 refers to the point on Stringer '9' midway between Frame 'C' and Frame 'D'.

2.2 The Loading System

The cylinder was mounted vertically between the machined faces of two heavy steel plattens (see Figs. 3,4, and 5). The compression load was applied by a 50 ton hydraulic jack mounted centrally on the upper platten and loading a tie-rod system screwed into the centre of the lower platten. Pressure was supplied to the jack by a hand-pump. The jack pressure gauge was calibrated to give the compression load on the cylinder.

2.3 Perturbation Loading

Outward (positive) and inward (negative) radial perturbation loads were applied to the cylinder by small dead weights acting through a double-ended bell-crank lever and a push-pull rod which engaged with the cylinder at certain points through special 4 BA bolts.

2.4 Instrumentation

(a) Longitudinal Compression

The contraction of the cylinder under load was measured along seven stringers equally spaced around the cylinder circumference. A small bracket was bolted externally near each end of the stringer. The relative movement of the lower bracket was then transmitted by a light alloy tube to a dial gauge rigidly mounted on the upper bracket (see Figs. 4 and 7).

(b) Stringer and Frame Deformation

The cylinder was surrounded by a scaffolding of seven steel pipes (see Figs. 4-8) to provide a convenient fixed structure for the attachment of dial gauges to measure the radial deflections of the cylinder.

Dial gauges were mounted at all frame-stringer intersections along the lengths of stringers 9 and 21.

The distortion of Frame 'C' was measured at most frame-stringer intersections around its circumference.

3. Test Procedure

3.1 Owing to irregularities in the end rings of the cylinder it was not possible to ensure an even distribution of load around the cylinder. In order to minimise the effects of uneven loading, the ends of the cylinder were shimmed until it was found that, under light load, increments of end load gave as nearly as possible equal increments in all the longitudinal compression gauge readings.

3.2 When the shimming was considered satisfactory, loading was commenced in increments of 100 lbs./sq.in. gauge pressure (approximately 1.8 tons) and three sets of readings were taken:

(a) The seven longitudinal compression gauges,

(b) The radial deflection gauges to determine the behaviour of stringers and frames under direct cylinder end load,

(c) The radial deflections of Stringer '9' and Frame 'C' under a series of radial perturbation loads up to 8 Kg. applied at points C9 and CD9.

As it was not possible to complete the tests in one day the load was removed for the night and a few check readings were taken before continuing the tests on the following day.

3.3 From the start of the tests, in spite of shimming, the compression gauge on stringer '20' had given a higher reading than the other compression gauges. It had been hoped that this might even out at higher loads, but at 17 tons compression this gauge was still reading 21 percent higher than the mean value for all seven gauges. The ends of the cylinder were even more heavily shimmed and a further series of tests was begun. It was still not possible to obtain even loading but the increased compression at Stringer '20' was decreased to about 7 percent of the mean compression at most cylinder end loads.

3.4 The previous tests were then repeated with the modification that the perturbation points were moved to C21 and CD21. As the failure was approached, (indicated by a marked reduction in the radial stiffness of the cylinder), the load was applied in smaller increments.

4. Results and Observations

4.1 Results of Tests

The development of buckling in the test cylinder is summarised in Table I.

The other test results have been presented graphically in Figs. 10-18.

The average and edge stresses in the skin were deduced from the applied compression load, the measured stringer contraction, and the measured cross-sectional areas of skin and stringers, assuming a value for Young's Modulus, E = 10,000,000 lbs./sq.in.

/4.2 ...

4.2 The Failure

When the cylinder end load exceeded 41,900 lbs. a marked falling off was observed in the stiffness of the cylinder against inward perturbation loads at CD21. From 43,900 lbs. this decrease in stiffness became even more evident as the perturbation gauges started to creep. Failure finally occurred at an end load of 45,900 lbs. when the cylinder was subjected to an inward perturbation load of 2 Kg.

The failure was of the " diamond" or " inward bulge" type and occurred on one side of the cylinder only, centred around Stringers 20, 21, 1 and 2 which had been shown by the longitudinal contraction readings to be the most heavily strained.

The buckled cylinder is shown in Figs. 7 and 8 while the final distorted shapes of the frames are shown in Fig. 9. The circumferential wave length of the failure was such as to have given five complete waves if fully developed.

In addition to the main buckles around the centre of the cylinder, subsidiary buckles, displaced one half wave length circumferentially, appeared over the lower part of the cylinder. The large number of flats, there should be ten, visible on Frame 'C' at failure (see Fig. 9) are due to the frame intersecting both the bottoms of the main central buckles and the tops of the bottom subsidiary buckles.

The wave forms of the stringers were dependent on their positions relative to the circumferential waves. Stringers which, as Nos. 1 and 21, passed through the middle of a main buckle, distorted as a built-in Euler strut (1 complete wave).

4.3 Correction of Experimental Critical Load

The failure occurred on one side of the cylinder only.

Assuming a linear variation of strain with end load for small changes in end load, then the observed failing load may be corrected to that for a fully developed General Instability failure by increasing it in the ratio of the maximum strain to the mean strain at failure.

On this assumption the observed critical load of 45,900 lbs. gives a corrected critical load of 50,000 lbs.

4.4 Comparison of Experimental and Calculated Results

The experimental and calculated loads are summarised in Table II.

The calculated results were very sensitive to the amount of skin effective. The effect on van der Neut's

/solution ...

solution of varying the effective skin is shown by the following figures:

(a)	with all skin effective	125,000 lbs.
(b)	with one-third of skin effective	81,800 lbs.
(c)	with effective skin as determined by test	52,800 lbs.

5. Discussion

5.1 The Normal Restraint Coefficient

In an extensive series of tests at the California Institute of Technology (Ref. 8) it was observed that there was a reduction in the normal restraint coefficient, or radial stiffness, as the load on the cylinder was increased. Measurement of the variation of the normal restraint coefficient might thus give a means of predicting the critical load from non-destructive tests.

From the plot of radial stiffness against compression load for the present test (see Fig. 11), it is readily seen that there is no simple law relating the radial stiffness to the load. As the compression load was applied to the cylinder the stiffness increased slightly at first and then gradually fell off until the initiation of skin buckling at a load of 31,000 lbs. The stiffness then became erratic, but remained substantially constant until a load of 41,000 lbs. was reached. Thereafter the stiffness fell off rapidly and the deflection gauges were observed to creep when inward perturbation loads were applied at CD21. The cylinder finally failed at 45,900 lbs. by inward bulging around the point of perturbation.

Thus the perturbation loading technique failed to predict the critical load from radial stiffness measurements at loads well below the critical.

However, provided the compression load is applied in small increments when nearing the critical load, perturbation loading may possibly be used to give a close indication of the approaching failure by observing the rapid decrease in stiffness and the onset of creep in the perturbation gauges. The percentage of load over which this warning occurs is, however, relatively small (about 10 percent in this test) and may be much less in many cases.

5.2 Deflections due to Compression Load

(a) Circumferential waves

From light load tests and up till failure it was observed that Frame 'C' was deflecting in a definite wave form (see Fig. 15) giving five complete circumferential waves, i.e. the same circumferential wave pattern as in the eventual General Instability failure. Probably, however, this effect was particularly marked due to the very light frames used. It may be a possible way of finding the circumferential wave length from non-destructive tests.

/(b) ...

(b) Longitudinal waves

Stringer deflections due to cylinder end load are shown in Figs. 12 and 13. The deflection pattern of Stringer '21', which passed through the main buckle at failure, was different at failure from that under light loads. Thus light load tests did not predict the longitudinal wave length at failure.

5.3 Perturbation Loading Deflections

(a) Circumferential waves

Under normal perturbation loads Frame 'C' distorted to give four complete circumferential waves superimposed on the five circumferential waves already caused by the cylinder end load (see Figs. 16 and 17); closer investigation, though, shows that the local perturbation wave length at the point of perturbation covered approximately four panel widths, giving a corresponding value of five complete circumferential waves. Perturbation loading may thus give another method for determining the circumferential wavelength.

(b) Longitudinal waves

Although direct compression loading of the cylinder did not indicate the longitudinal wave form at failure, the deflections due to perturbation alone (see Fig. 14) were of the same built-in Euler strut pattern as at failure. Hence perturbation loading may also be of use in determining the longitudinal wave length.

5.4 Agreement with Theoretical and Empirical Formulae

5.4.1. Of the available formulae dealing with the General Instability problem, those due to van der Neut (Ref. 6) and Hoff (Ref. 4) gave very good agreement with the test result, but it must be noted that in both cases the solution of the equations was dependent on certain test information.

5.4.2. Van der Neut's second equation was used. This assumes discrete equally spaced frames but uniformly distributed stringers. As van der Neut points out, his equation yields 2^2 possible critical loads corresponding to all the various combinations of longitudinal and circumferential wave length. The minimum value of all these loads gives the actual failing load. Van der Neut indicates a way of obtaining a solution, but this is handicapped at present by lack of accurate knowledge of load-carrying capabilities and stiffness of curved skin panels after buckling.

The given solution to van der Neut's equation was dependent on the test values of circumferential and longitudinal wave lengths and on the average to edge stress relationship for the buckled skin panels. The effect of incorrect assumptions of the effective widths of skin is shown by the results in paragraph 4.4. Assuming the skin was one-third effective, the critical load was overestimated by more than 60 percent. Actually, the tests showed that at the critical load the skin was ineffective for stiffness and 0.57 effective for load carrying.

/5.4.3. ...

5.4.3. Hoff's revised semi-empirical equation (Ref. 4) for the General Instability of a cylinder in bending was applied to the test cylinder using the experimental values for the circumferential wave length. Agreement on the critical load was very good but there are some discrepancies in other figures.

For the determination of n (half the number of circumferential waves) Hoff gives a set of curves (Ref. 4, Fig. 10) derived from experimental results on cylinders in bending. The test cylinder fell outside Hoff's range of values but extrapolation of the curves gives n = 4, i.e. eight circumferential waves, and a corresponding critical load of 87,000 lbs. Cf. test values of five circumferential waves and a critical load of 50,000 lbs. The difference may be due to Hoff's results applying strictly only to bending, whereas the test was made in pure compression.

Hoff's formula also indicates a maximum strain at failure of 0.00126 compared with a measured strain of 0.00112. The difference is probably largely due to inaccuracies in the effective width of skin as determined from a modified form of Marguerre's cube root formula. Hoff, himself, states that this formula is not reliable, but that no better method is known to him.

5.4.4. Dunn's empirical formula (Ref. 7) derived from the results of the GALCIT tests (Ref. 8) overestimated the critical load by 19 percent using his suggested values for the effective skin and by 14 percent using the experimental values for effective skin. Owing to the extremely complex nature of the General Instability problem, it is considered that Dunn's equation may have oversimplified the parameters involved; though it may hold for the small scale cylinders used in the GALCIT tests, its veracity is doubtful when applied to larger cylinders, particularly of the sizes where General Instability becomes a practical problem in aircraft structural design.

5.4.5. Taylor's theory (Ref. 2) gave an imaginary solution when applied to the test cylinder. This equation is one of the earliest attempts to solve the General Instability problem and takes no account of some important variables.

6. Conclusions

1. The Normal Restraint Coefficient

The normal restraint coefficient (radial stiffness) cannot be used to predict the critical load for a thin stiffened metal cylinder under compression. The change of stiffness with end load is not according to any simple law and there is a sudden drop in stiffness as the critical load is approached.

However, with care, a non-destructive test may be made by measuring the radial stiffness while increasing the compression load, and observing the sudden decrease in stiffness as the failure approaches. In the test this drop in stiffness occurred at 90 percent of the critical load, while at 96 percent the cylinder was observed to creep under perturbation loads.

/2. ...

2. Prediction of the Circumferential and Longitudinal Wave Lengths of Buckling

It was possible to predict both the buckling wave lengths from non-destructive tests.

Measurements of the cylinder distortion under radial perturbation loads predicted both the circumferential and the longitudinal wave lengths.

Measurements of the cylinder distortion under relatively light compressive end loads predicted the circumferential wave length, but was not successful in predicting the longitudinal wave length.

3. Comparison with Critical Loads from Theoretical and Empirical Formulae

(a) Van der Neut's second equation gave good agreement on using experimental values for the circumferential and longitudinal wave lengths and for the skin average and edge stresses.

(b) Hoff's revised formula agreed closely using experimental circumferential wave length instead of that read off his chart.

(c) Dunn's empirical law overestimated the critical load and is considered unlikely to yield reliable results in general.

(d) Taylor's equation gave an imaginary failing load and is not satisfactory.

4. Stresses in Curved Skin Panels

For further progress in the General Instability problem it is essential to have relaible information on the stresses and stiffness of curved skin panels after buckling.

--ooOoo--

REFERENCES

No.	Author	Title, etc.
1.	Grant, H.B.	Tests on the General Instability of Stiffened Circular Cylinders. Thesis, College of Aeronautics, 1948.
2.	Taylor, J.L.	The Stability of a Monocoque in Compression. A.R.C. Reports and Memoranda 1679, 1935.
3.	Hoff, N.J.	Instability of Monocoque Structures in Pure Bending. Jour. Roy. Aero. Soc., Vol. 42, pp. 291-346, April 1938.
4.	Hoff, N.J.	General Instability of Monocoque Cylinders. Jour. Aero. Sci., Vol. 10, pp. 105-114; 130, April 1943.
5.	Cox, H.L.	Stress Analysis of Thin Metal Construction. Jour. Roy. Aero. Soc., Vol. 7, pp. 231-282, March 1940.
6.	Van der Neut, A.	The General Instability of Stiffened Cylindrical Shells under Axial Compression. Nationaal Luchtvaartlaboratorium, Report S.314, October 1946.
7.	Dunn, Louis G.	Some Investigations of the General Instability of Stiffened Metal Cylinders. IX - Criterions for the Design of Stiffened Metal Cylinders Subject to General Instability Failures. NACA Technical Note No.1198, November 1947.
8.	Guggenheim Aeronautical Laboratory, California Institute of Technology.	Some Investigations of the General Instability of Stiffened Metal Cylinders. NACA Technical Note Nos. 905-909. 1943.

T A B L E I

Development of Buckling in the Test Cylinder

Load	Av. Stress	Str gr. Stress	Av. Skin Stress	Remarks
Lbs.	P.s.i.	P.s.i.	P.s.i.	
23,110	4,500	4,955	4,230	'Inter-bolt buckling'.
31,000	6,040	6,700	5,640	Skin Buckling began.
42,900	8,370	10,590	6,980	Skin Buckling becoming general.
43,900	8,560	10,960	7,060	Gauges showed tendency to creep under inward perturbation loads at CD21.
44,900	8,755	11,470	7,060	Gauges showed marked creeping under inward perturbation loads at CD21.
45,900	8,950	12,140	6,955	General Instability Failure under 2 Kg. inward perturbation load at CD21.

T A B L E II

Comparison of Experimental and Calculated Results

Derivation	Critical Load (lbs.)
Test cylinder:- (a) Uncorrected result. (b) Corrected result.	45,900 50,000
Van der Neut :- Using experimental values for longitudinal and circumferential wave lengths and for relation between skin average and edge stresses.	52,800
Hoff's Revised Theory:- (a) Using extrapolated value from Hoff's chart of n = 4. (b) Using experimental value for the circumferential wave length (n=2.5)	87,000 49,400
Dunn:- (a) Using Dunn's values for the effective widths of skin. (b) Using experimental values for effective widths of skin.	59,600 56,900
Taylor	Imaginary solution.

LIST OF FIGURES

FIG. 1.

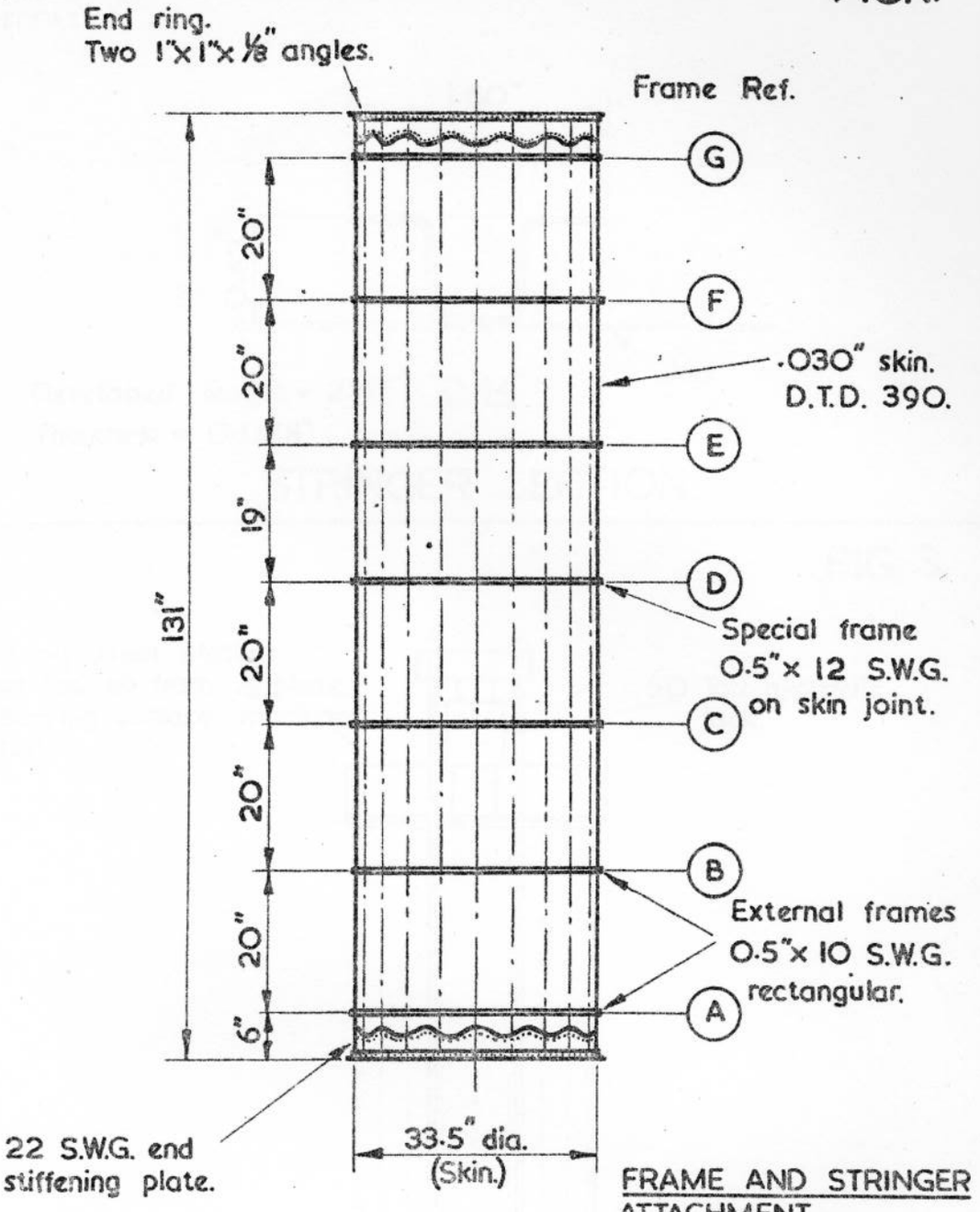

FRAME AND STRINGER ATTACHMENT

4 B.A. bolts at approx. 0.75" pitch.

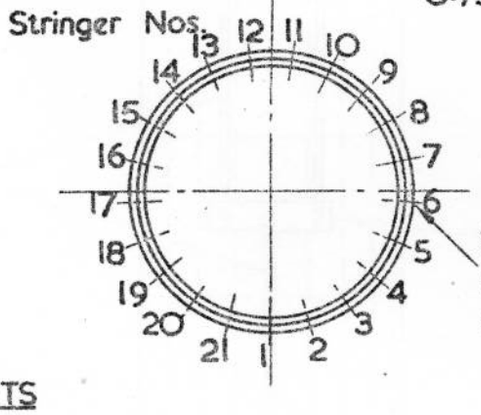

SKIN JOINTS

1. All simple lap joints.
2. Circumferential joint at frame 'D'.
3. Longitudinal joints at stringers Nos. 1, 8 and 15.

G.A. OF CYLINDER.

FIG. 2.

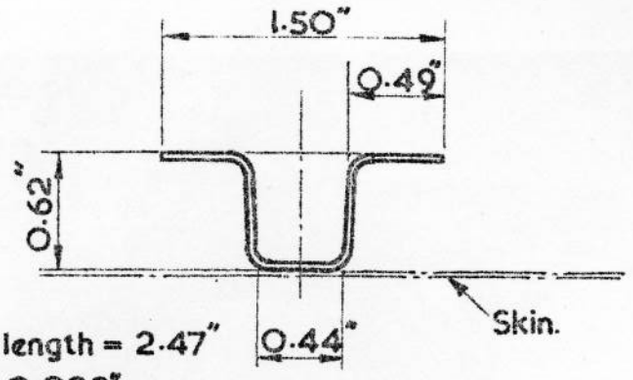

Developed length = 2.47"
Thickness = 0.038"

STRINGER SECTION.

FIG. 3.

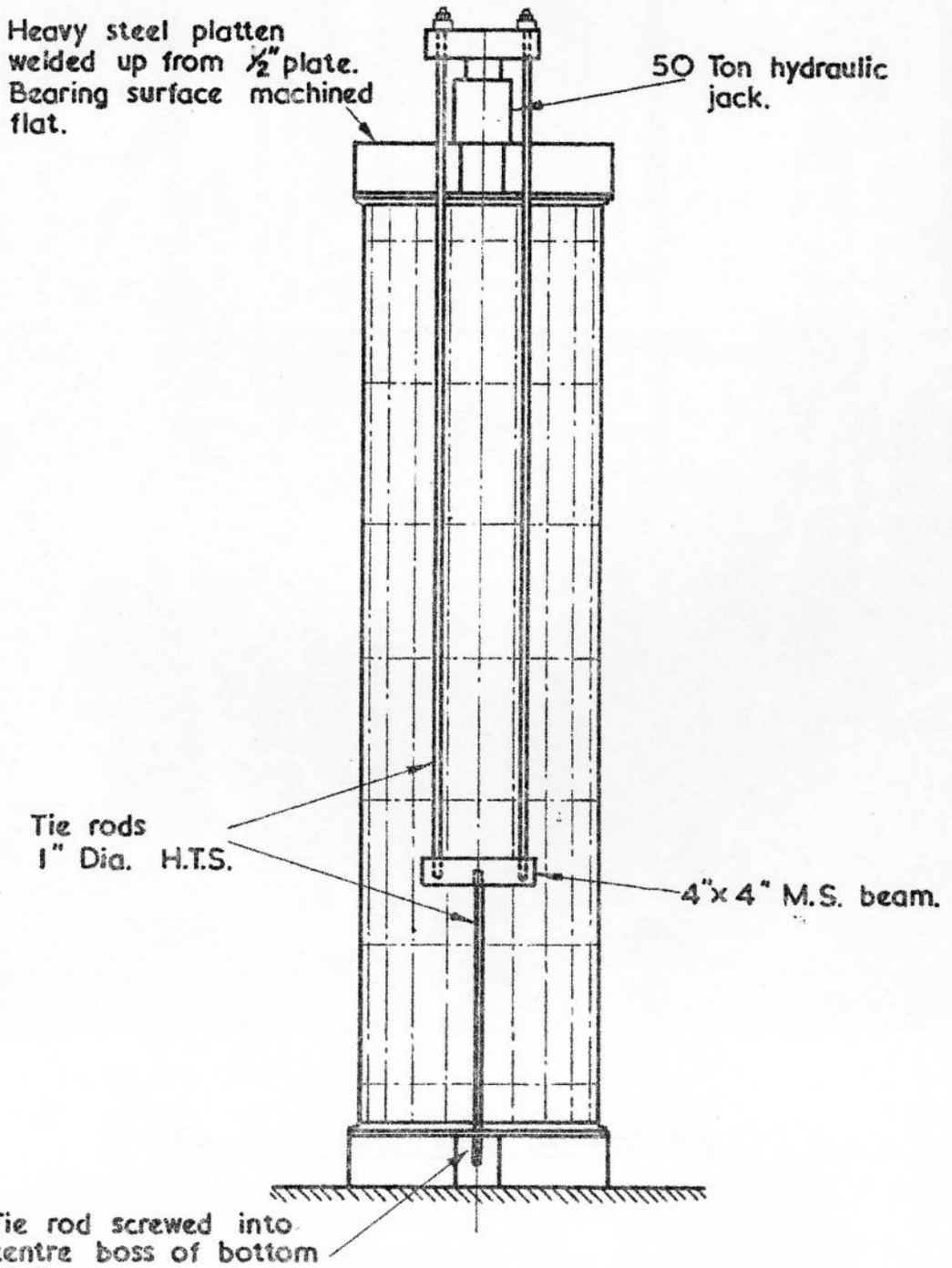

SECTIONED G.A. OF LOADING SYSTEM.

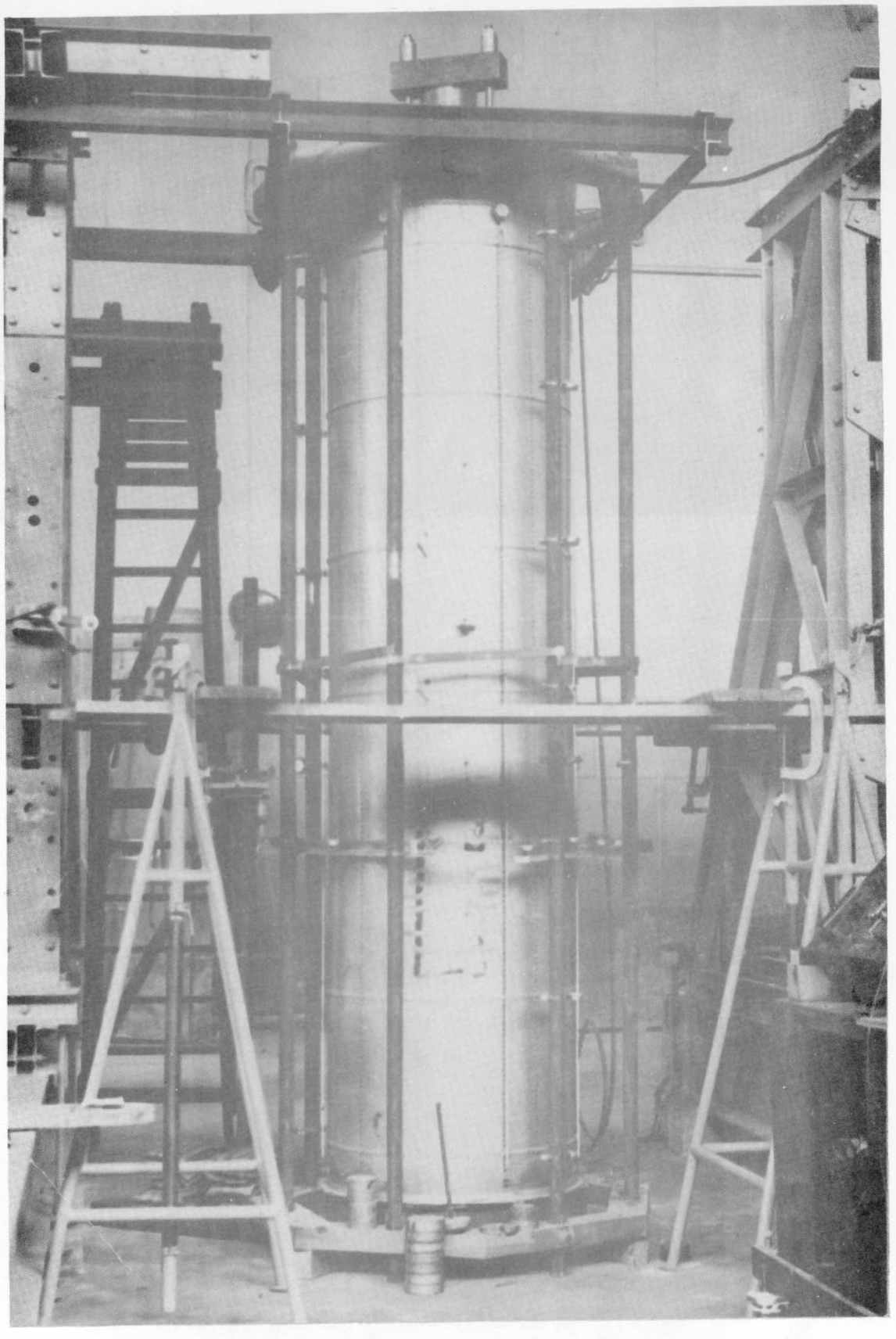

Fig 4 General View of Test Rig

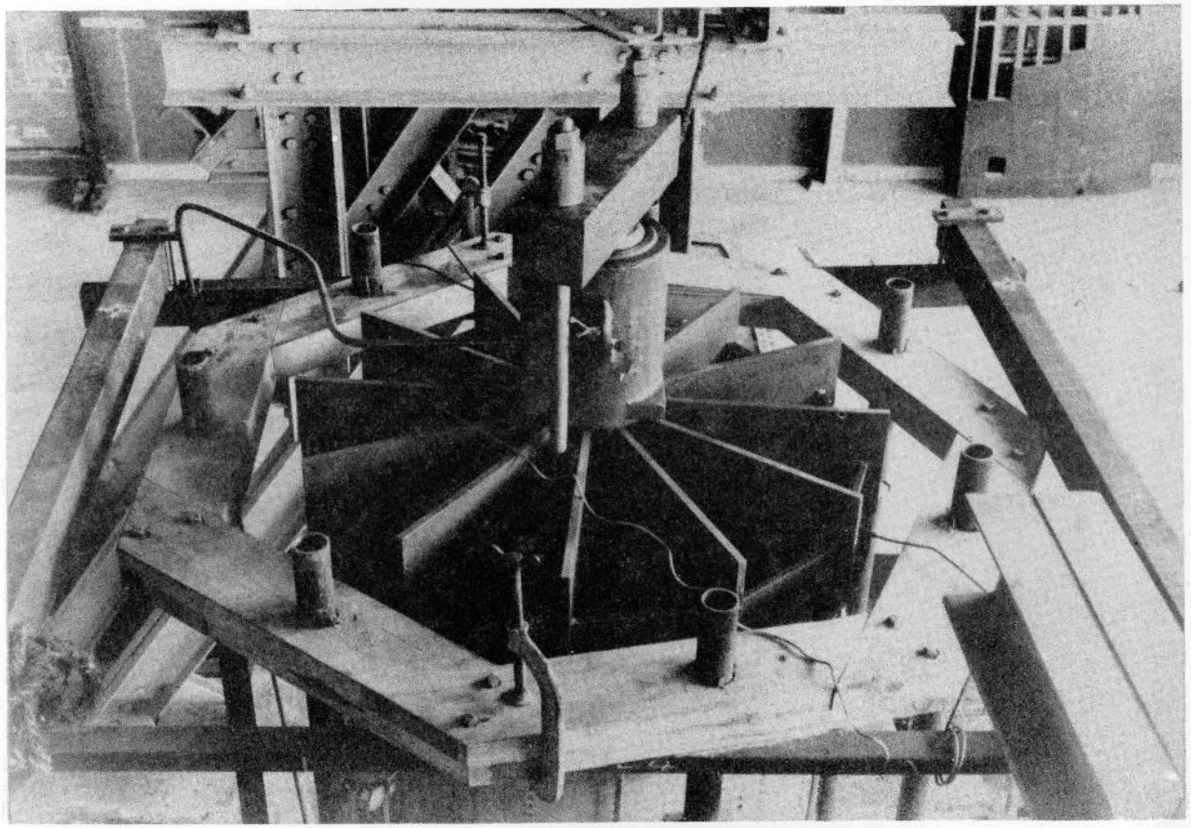

Fig 5 View of Ram Top Platten and

Top of Gauge Support Scaffolding

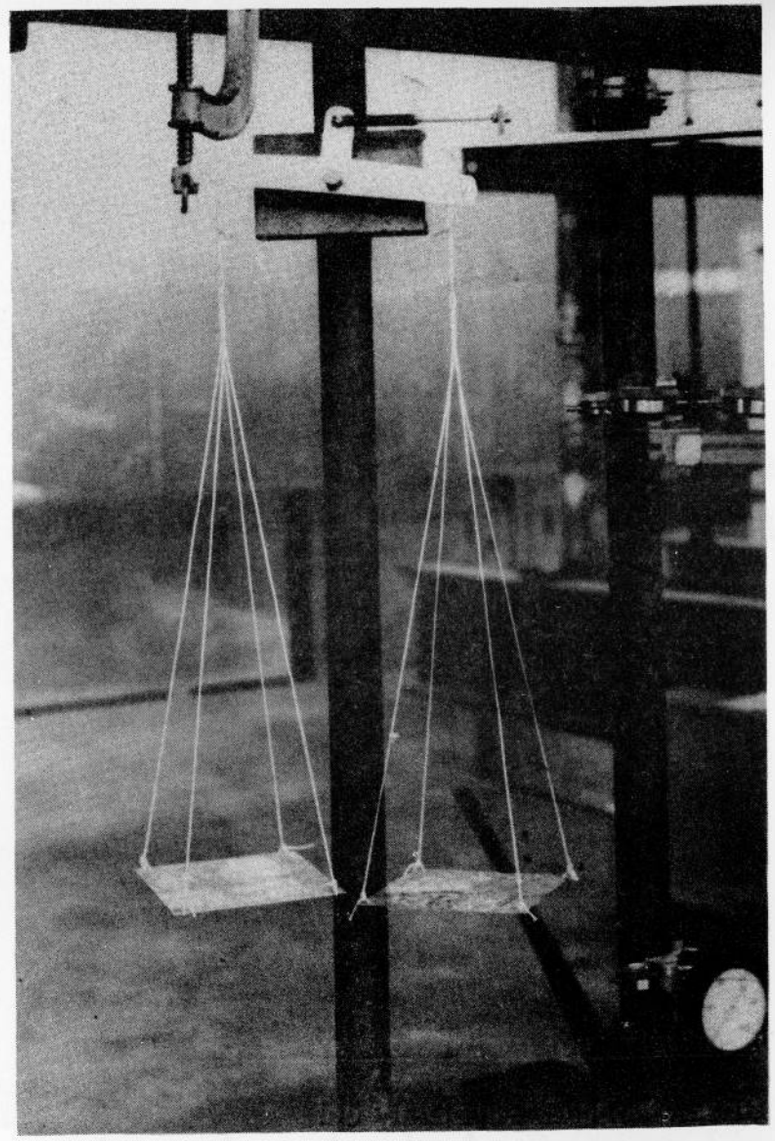

Fig 6 Radial Perturbation Mechanism

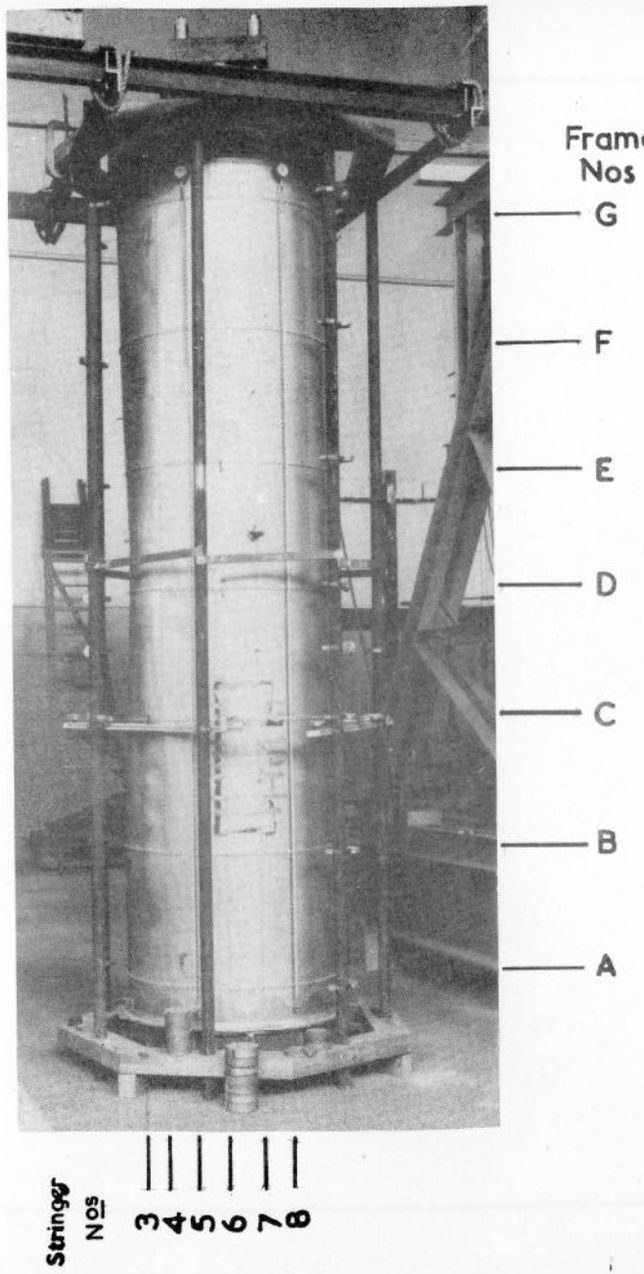

Fig 7
Side on View
of Main Buckle

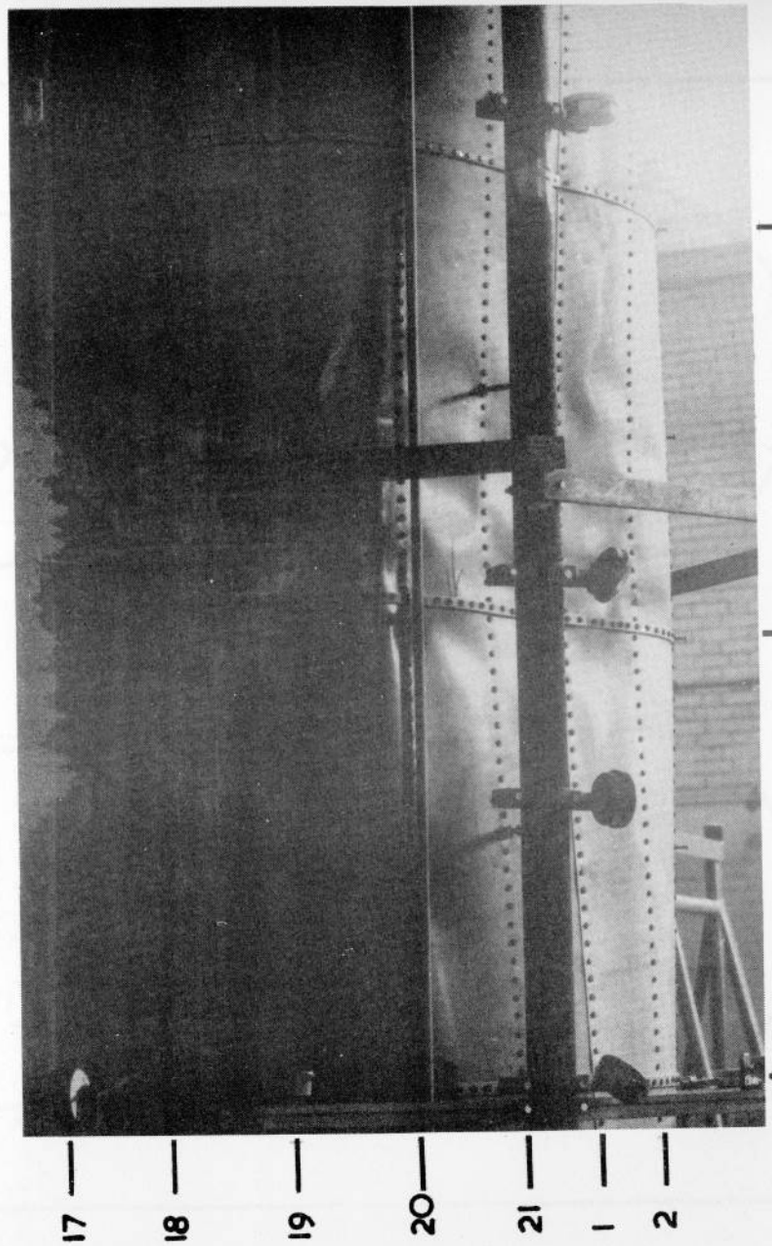

Fig 8
Close up of
Main Buckle

FIG.9.

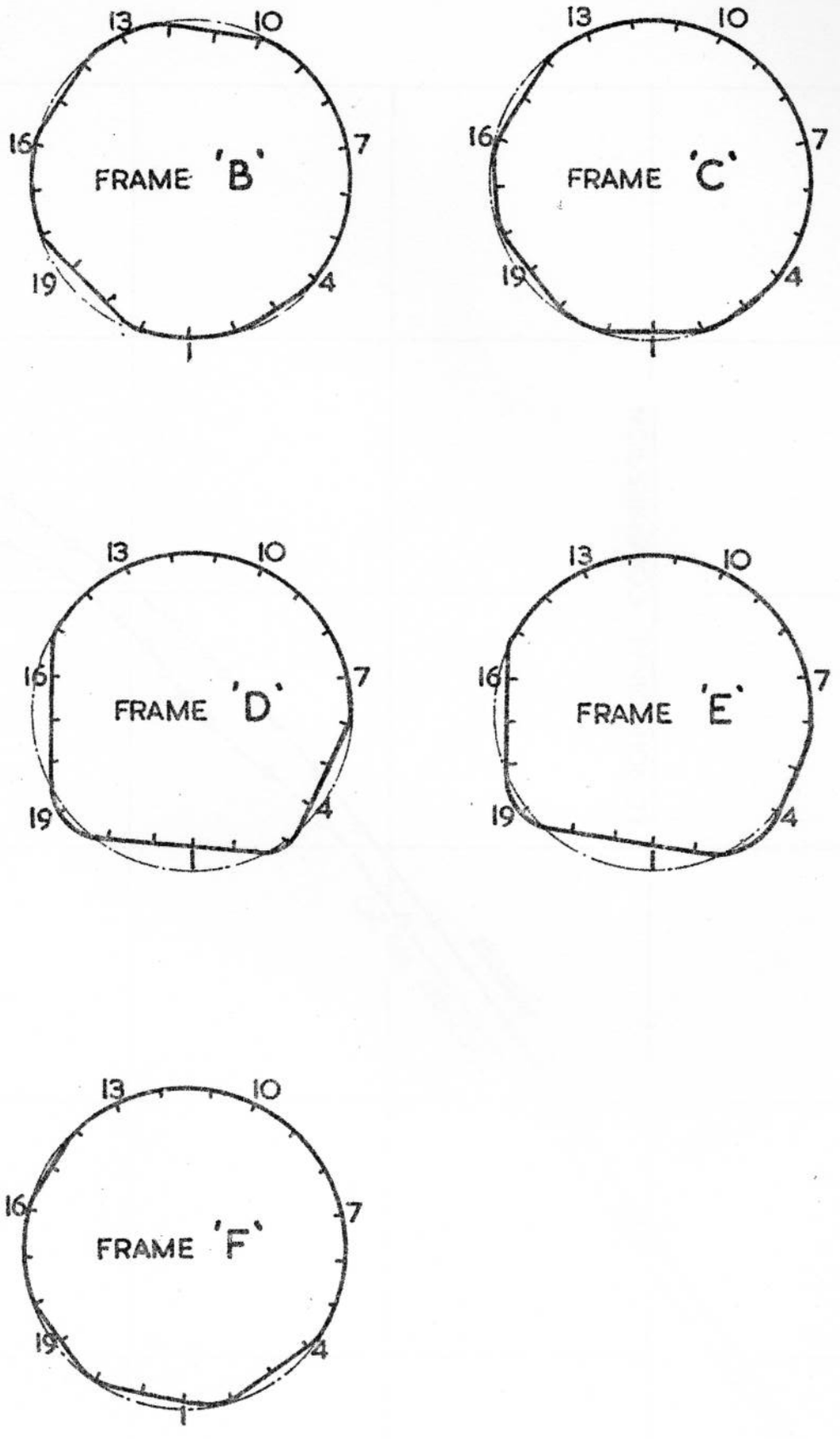

DISTORTION OF FRAMES IN GENERAL INSTABILITY FAILURE.

FIG 10

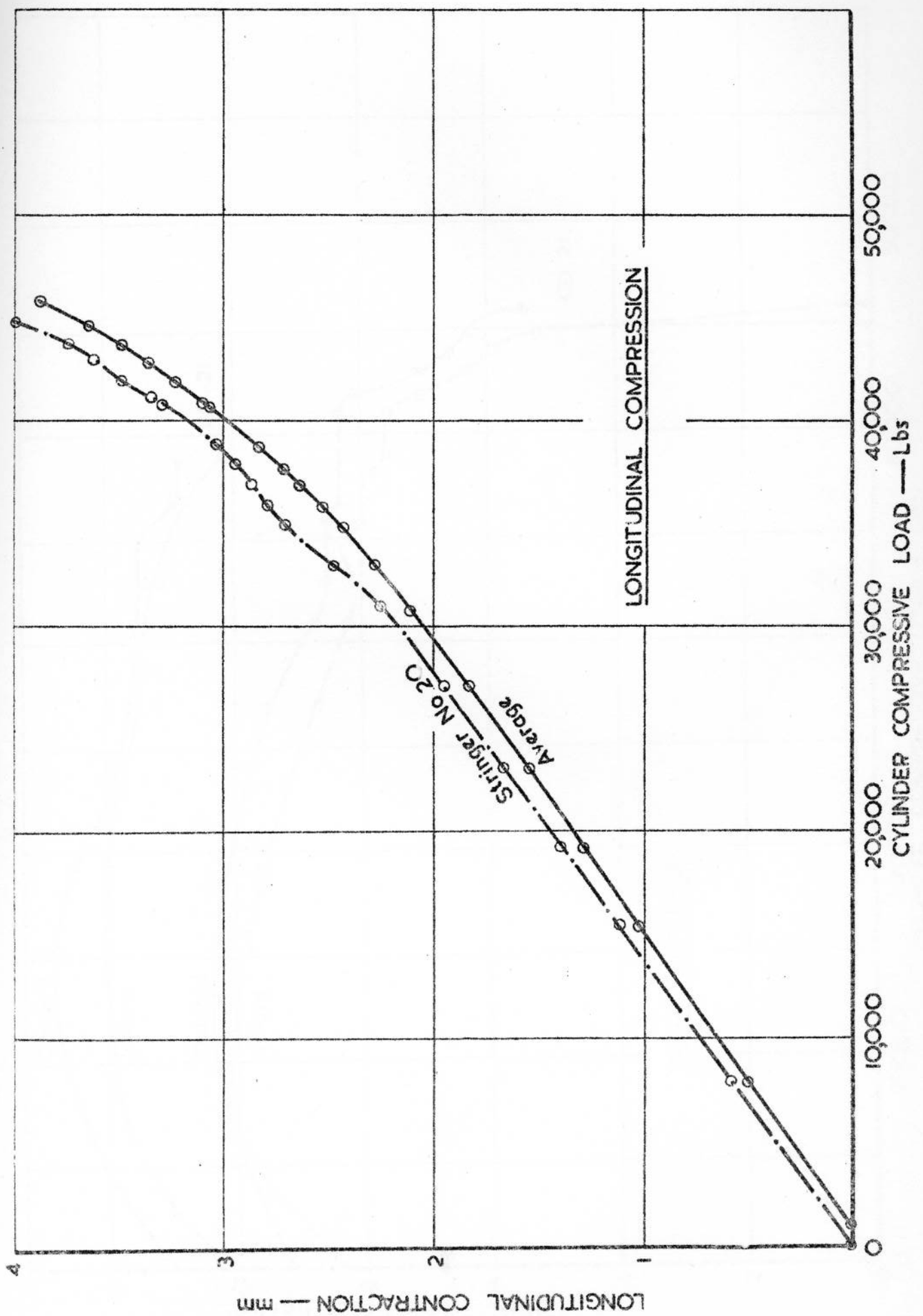
LONGITUDINAL COMPRESSION
Stringer No 20
Average
CYLINDER COMPRESSIVE LOAD — Lbs
0
10,000
20,000
30,000
40,000
50,000
LONGITUDINAL CONTRACTION — mm
1
2
3
4

FIG. 11.

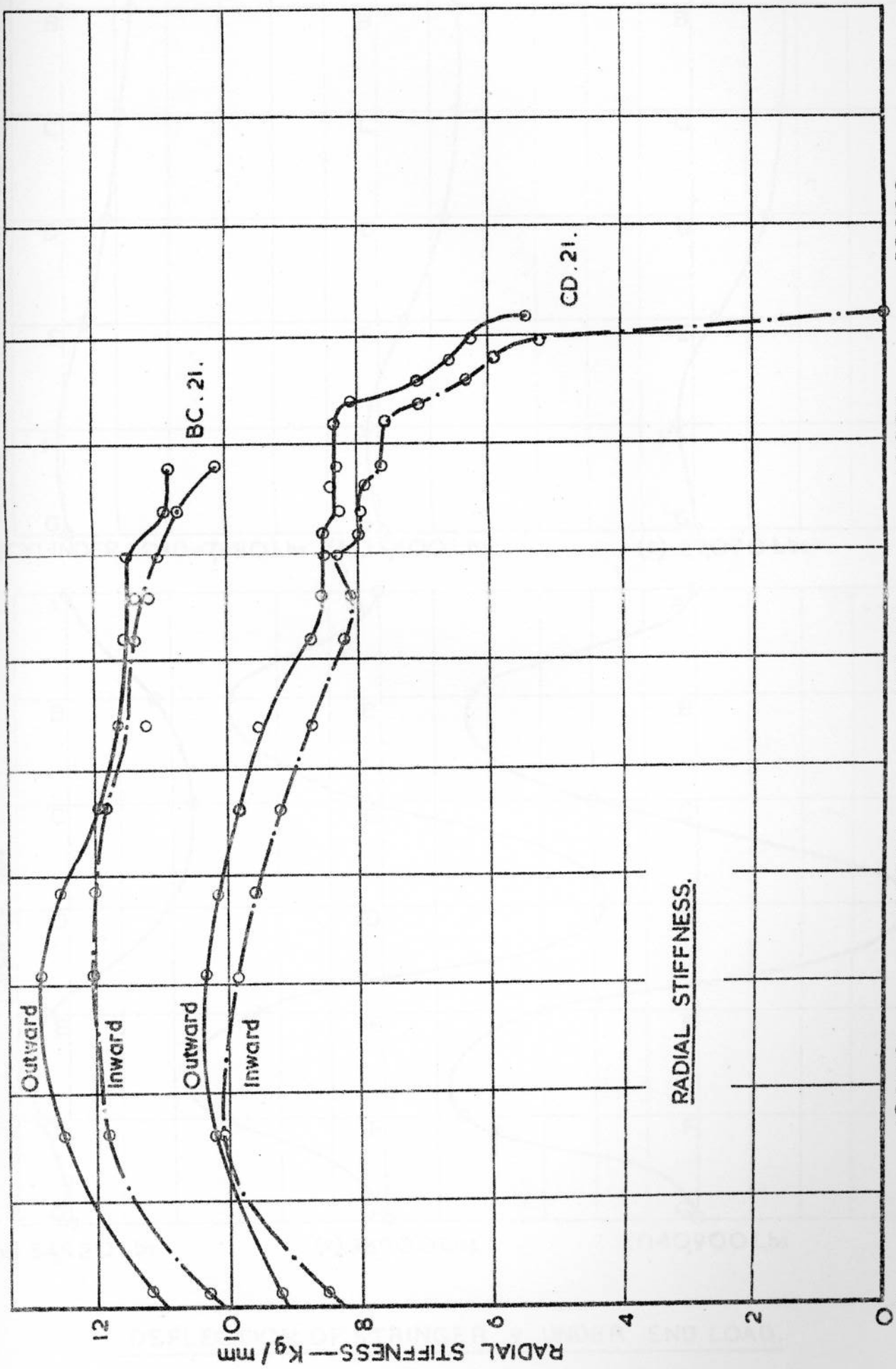
RADIAL STIFFNESS.
BC. 21.
CD. 21.
Outward
Inward
Outward
Inward
RADIAL STIFFNESS — Kg/mm
12
10
8
6
4
2
0
0
10,000
20,000
30,000
40,000
50,000
CYLINDER COMPRESSIVE LOAD — LBS.

FIG.12.

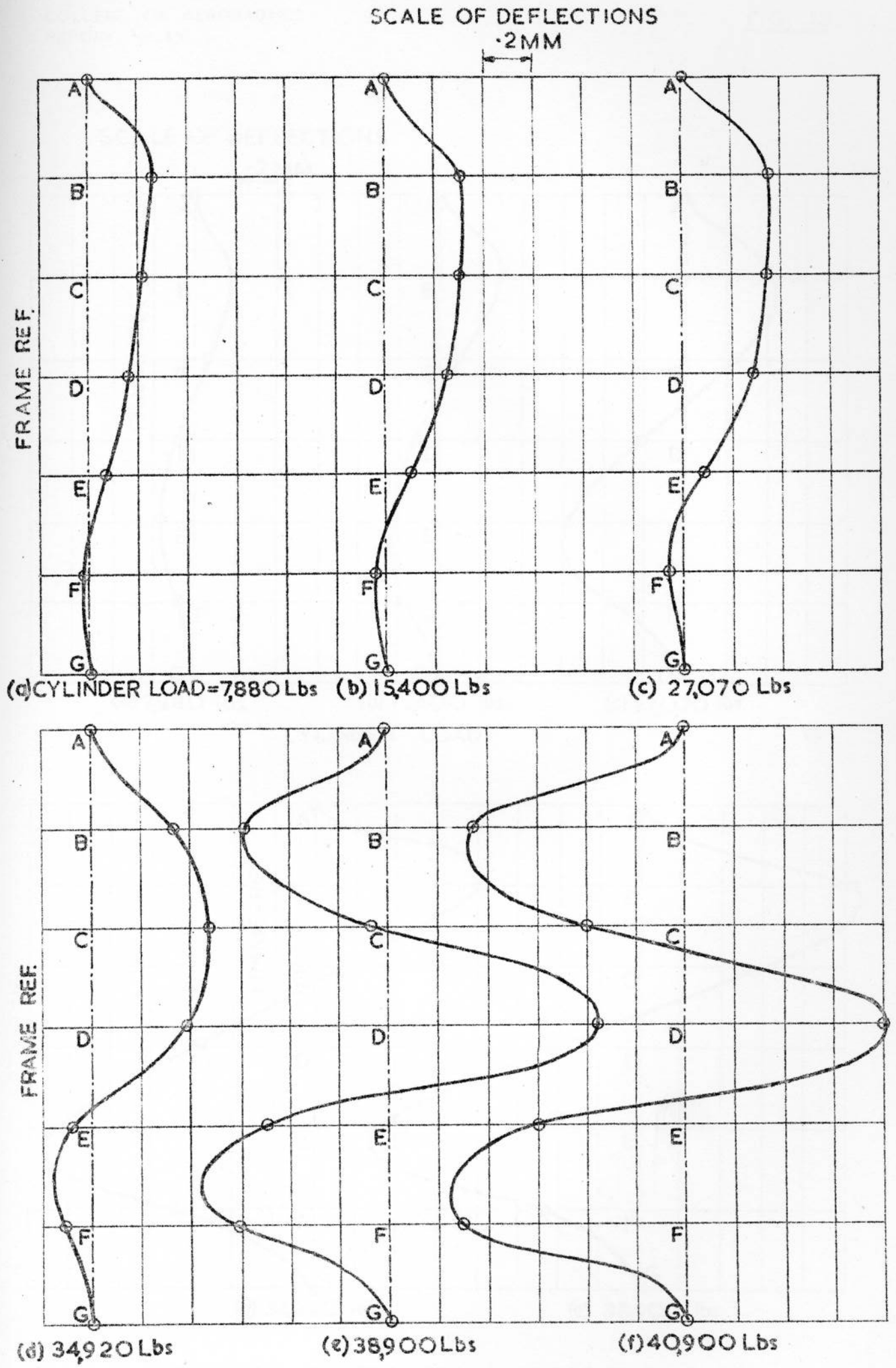

DEFLECTION OF STRINGER 9 UNDER END LOAD.

FIG. 13.

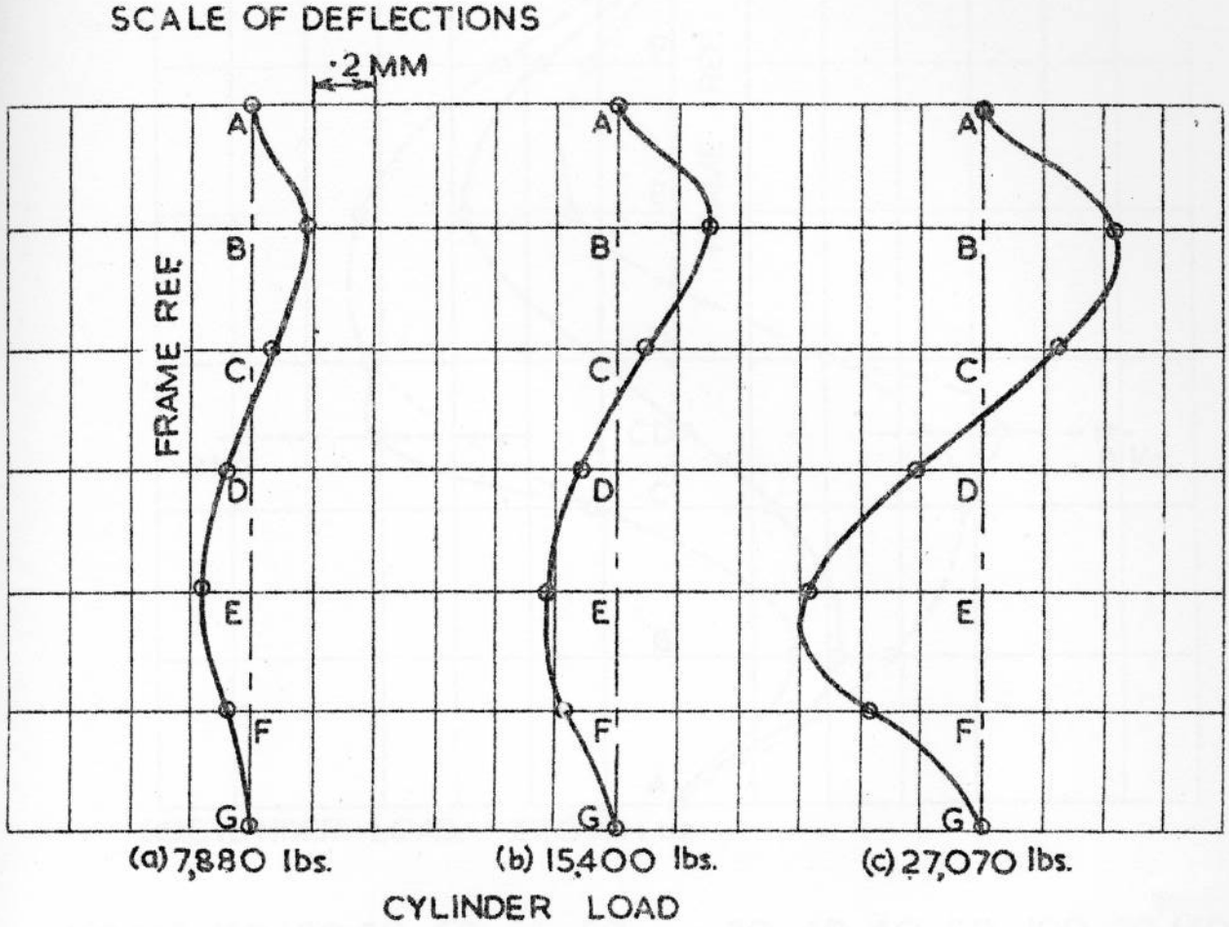

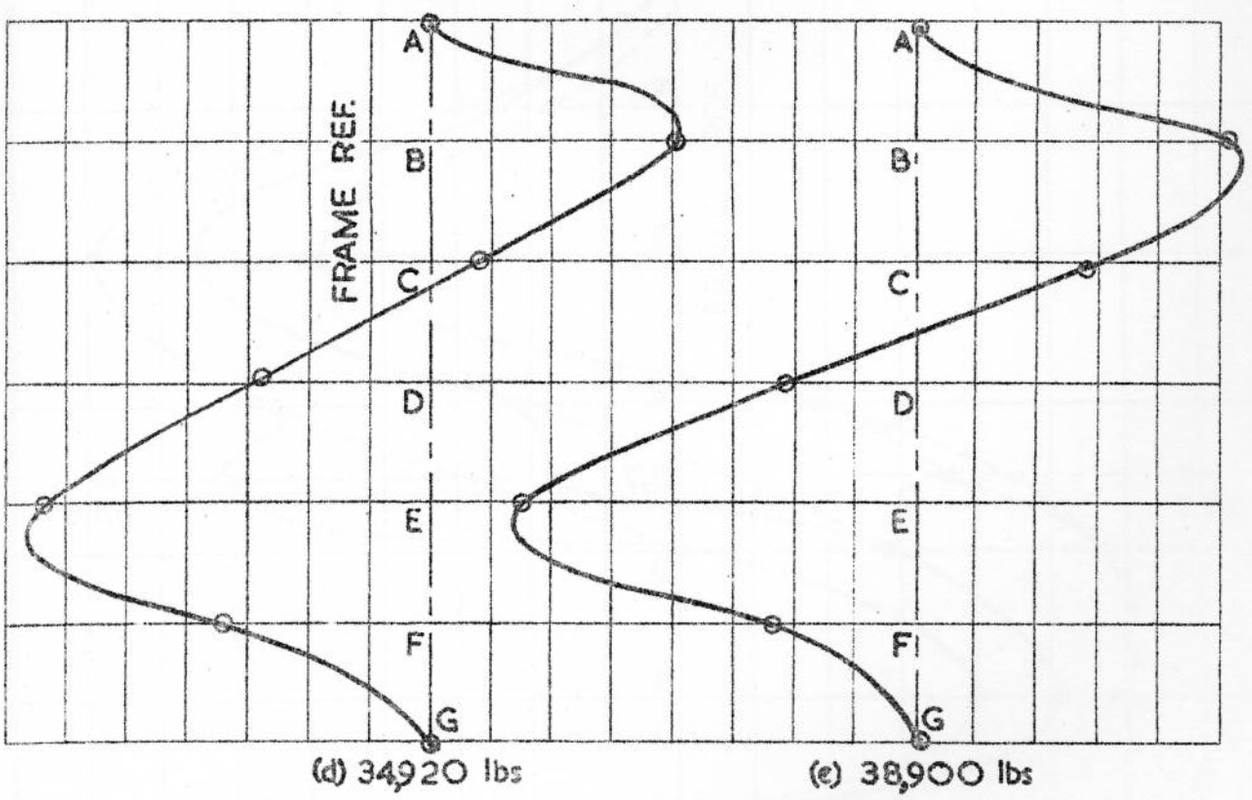

DEFLECTION OF STRINGER 21 UNDER END LOAD.

FIG. 14.

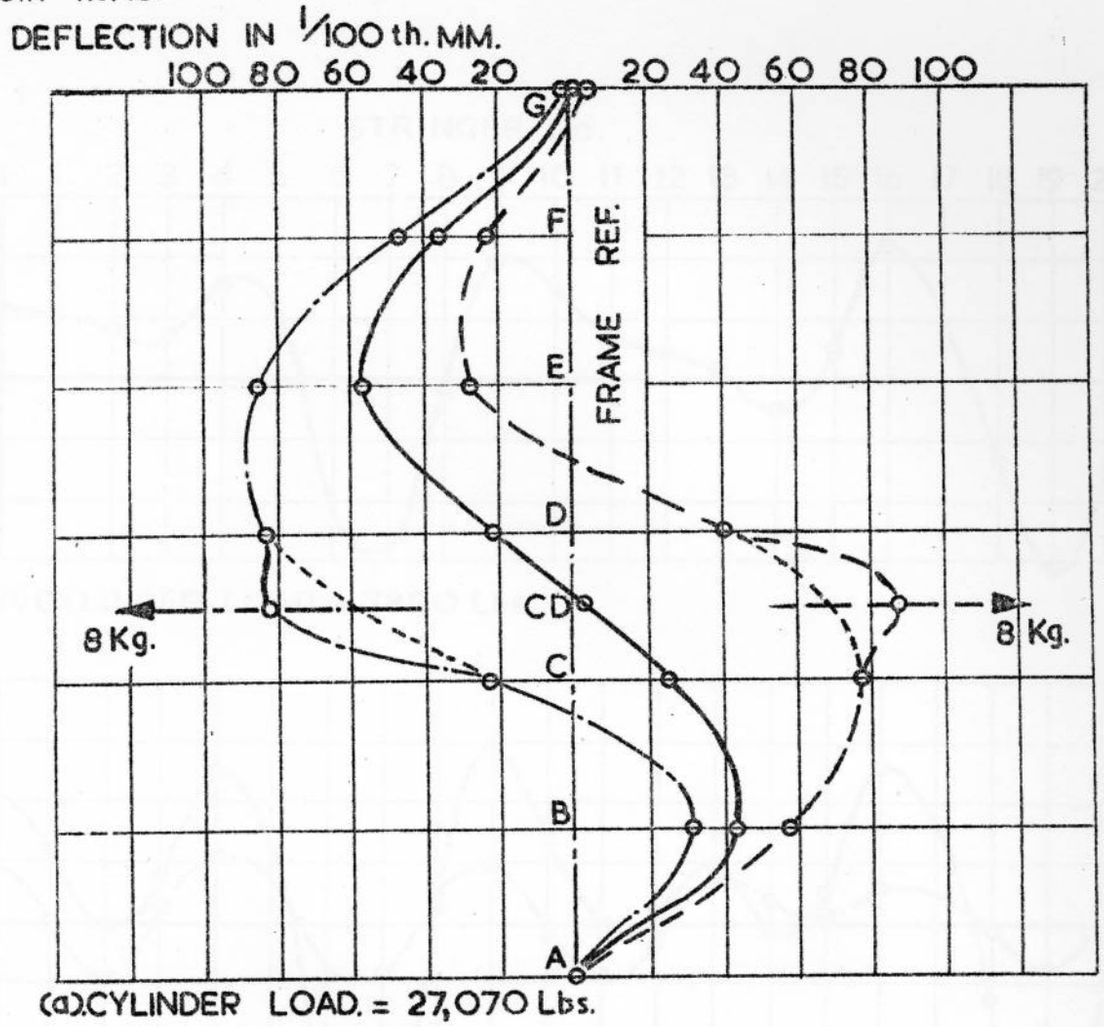

(a). CYLINDER LOAD. = 27,070 Lbs.

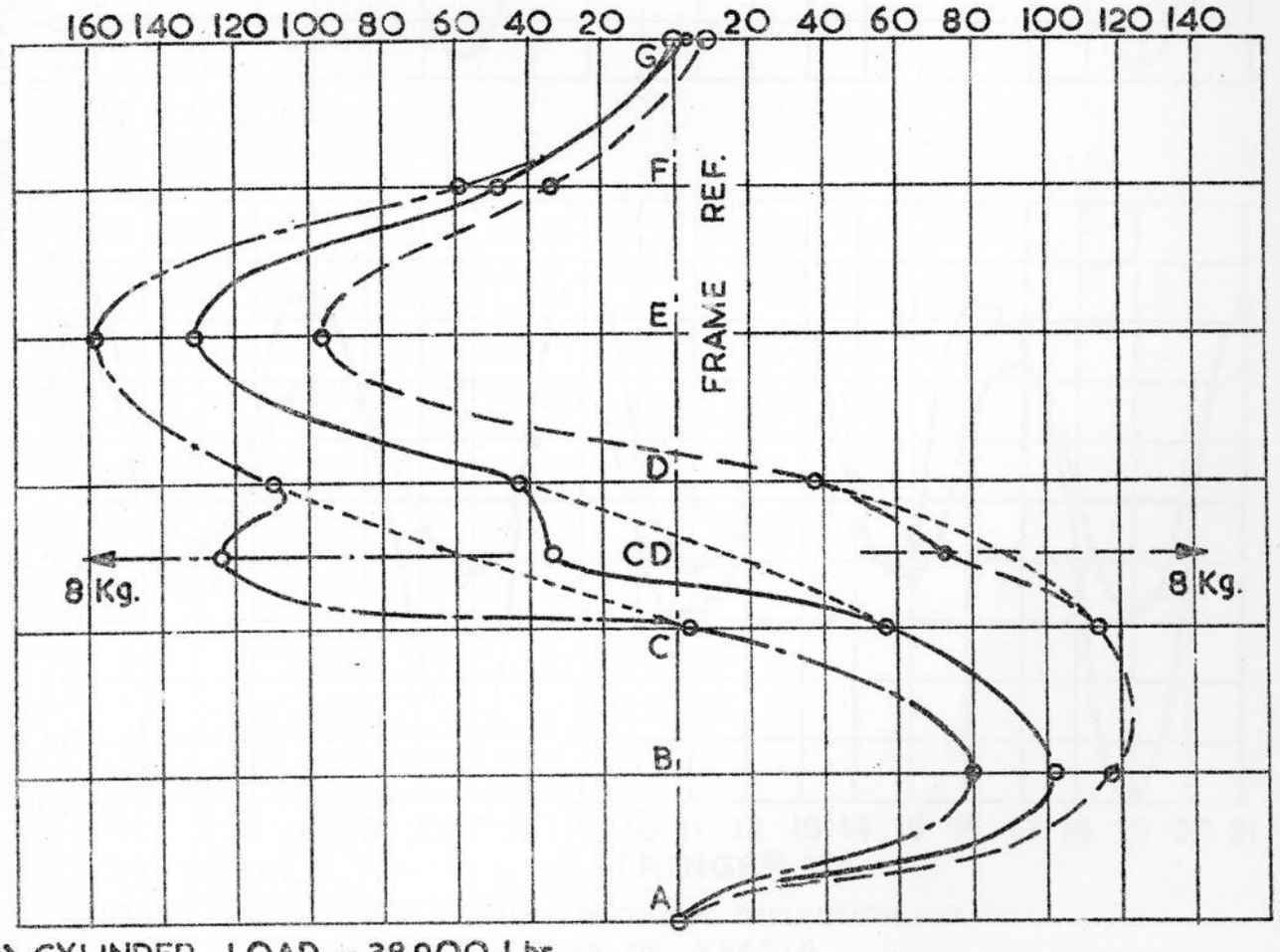

(b) CYLINDER LOAD = 38,900 Lbs.

DEFLECTION OF STRINGER 21 UNDER PERTURBATION LOAD.

FIG. 15.

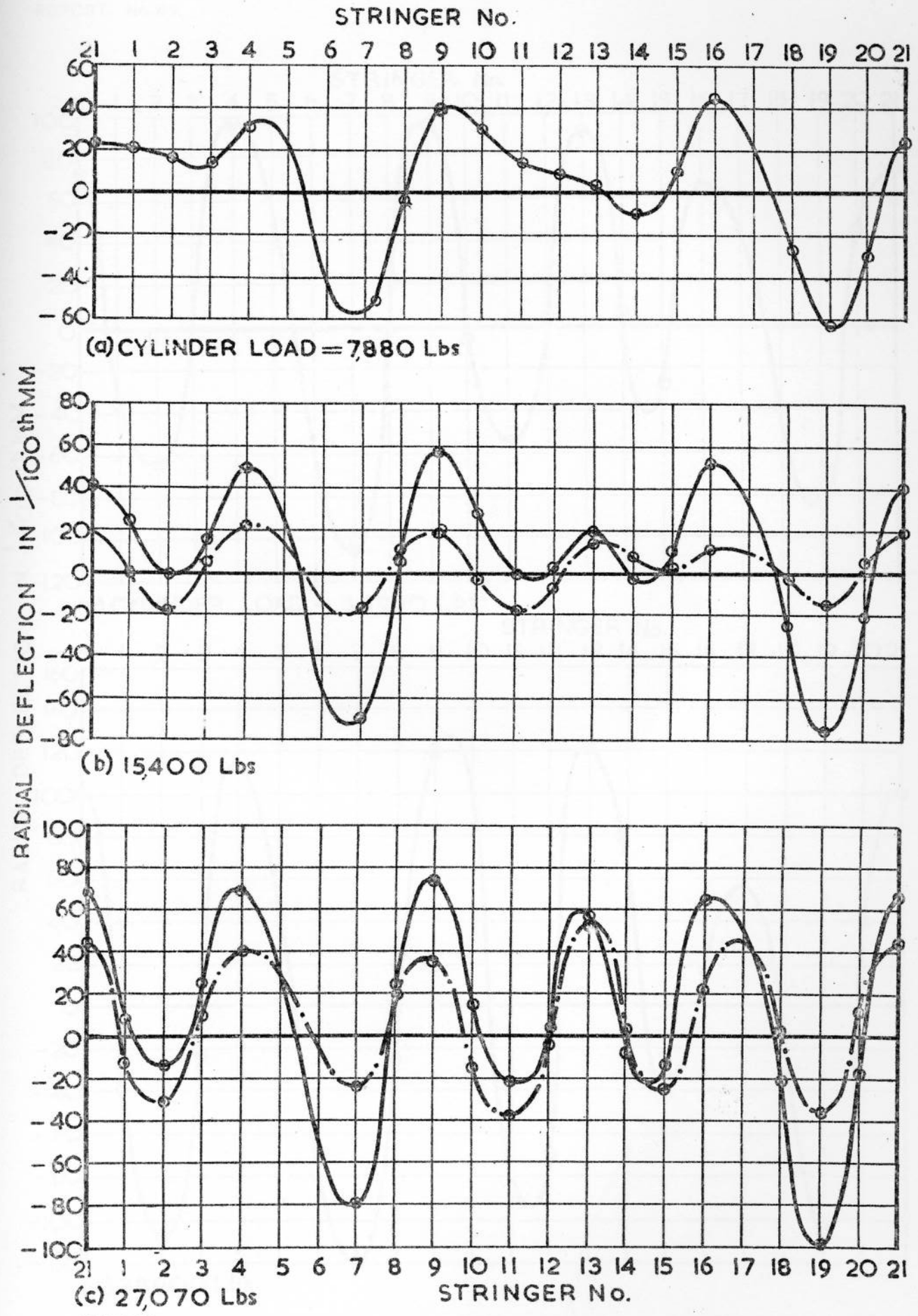

NOTE: —·— TRACE SHEWS ADDITIONAL DEFLECTION DUE TO LOAD IN EXCESS OF 7880 Lb

DEFLECTION OF FRAME 'C' UNDER CYLINDER END LOAD.

FIG 15 (CONT).

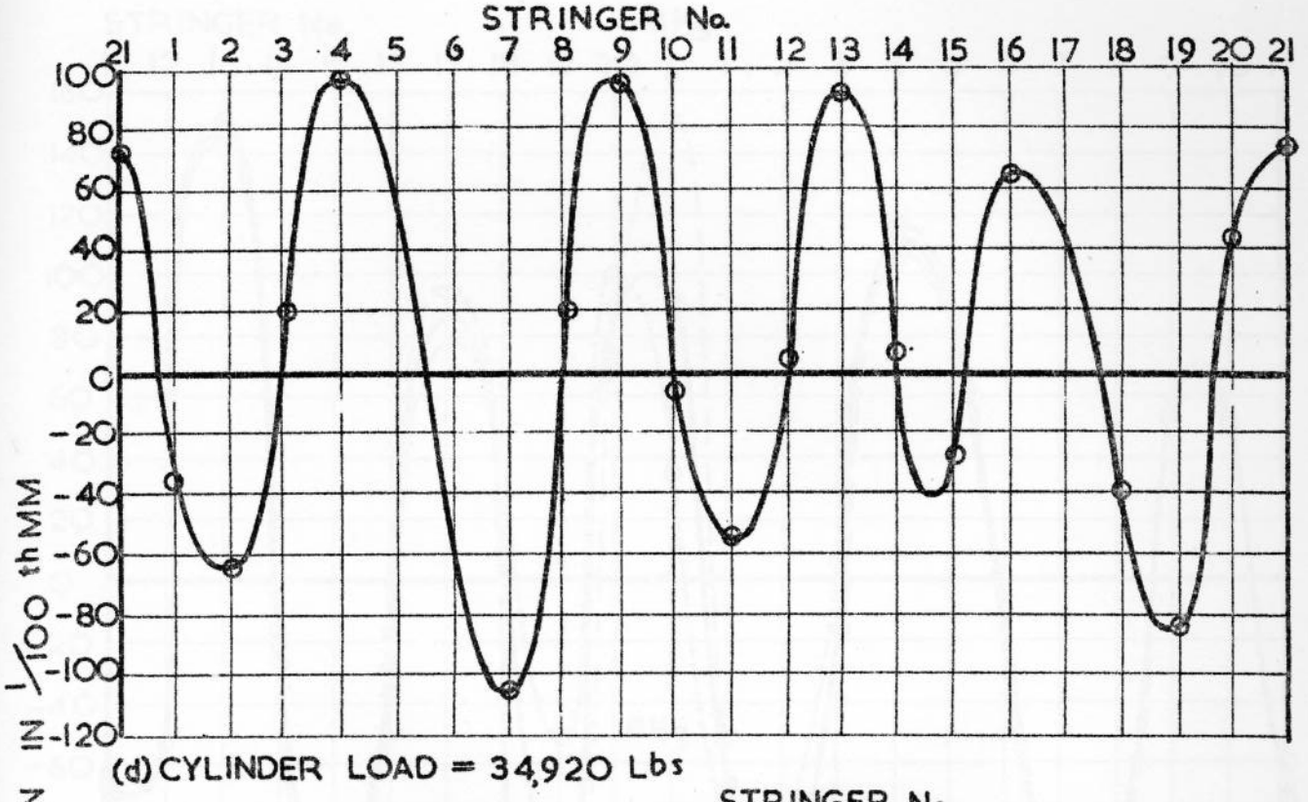

(d) CYLINDER LOAD = 34,920 Lbs

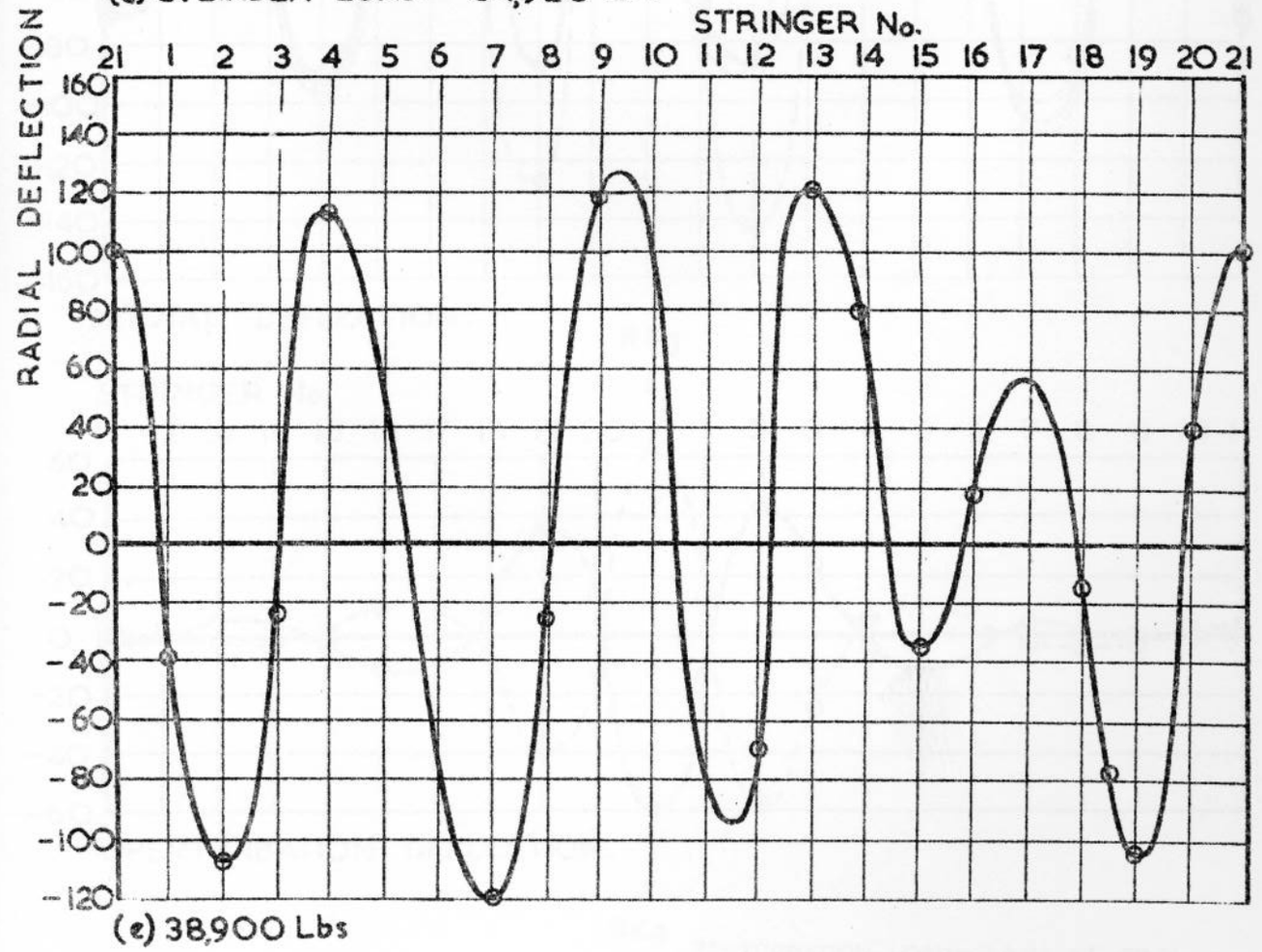

(e) 38,900 Lbs

DEFLECTION OF FRAME 'C' UNDER CYLINDER END LOAD.

FIG. 16.

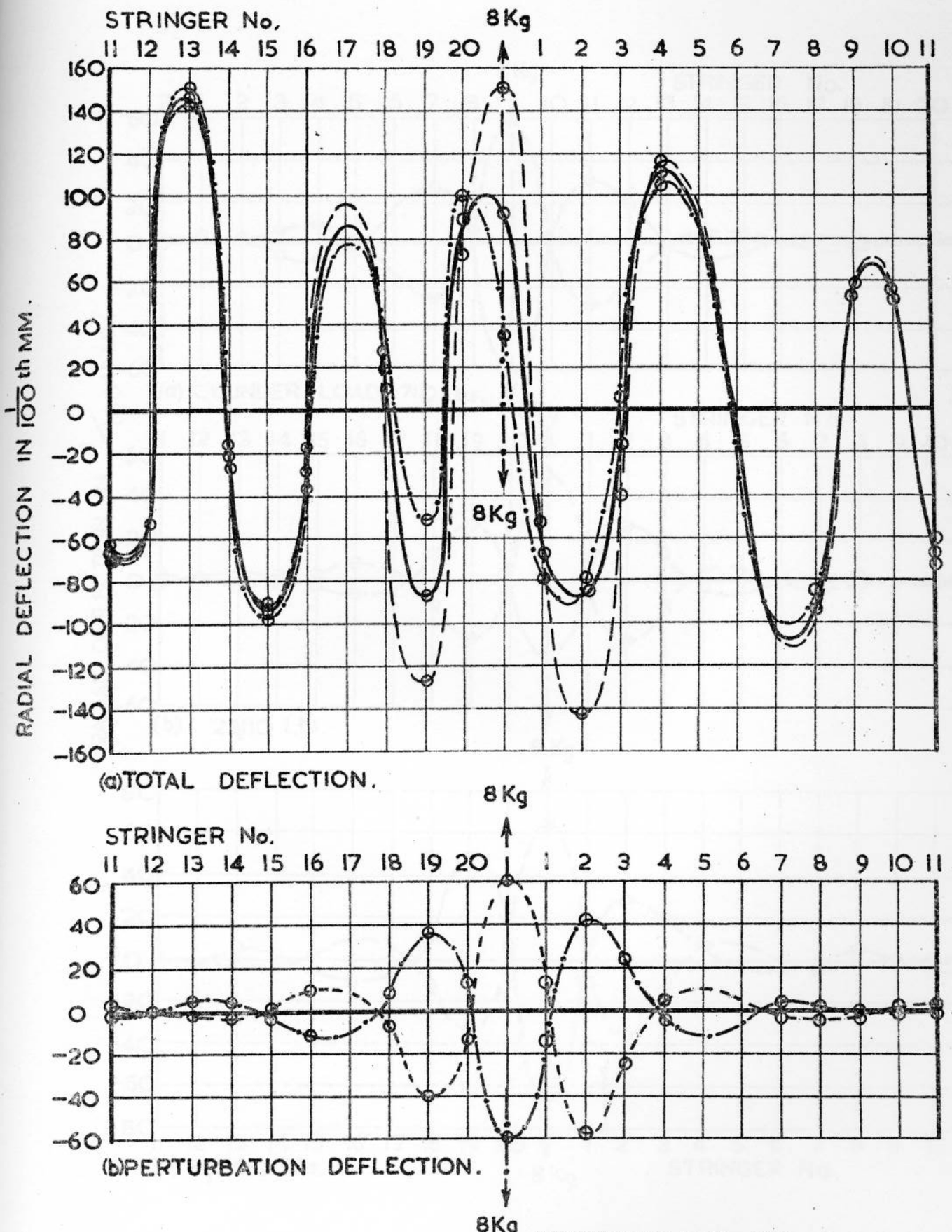

PERTURBATION LOAD = ±8 Kg AT CD 21
CYLINDER LOAD = 38,900 Lbs

DEFLECTION OF FRAME 'C' UNDER PERTURBATION LOADS.

FIG . 17.

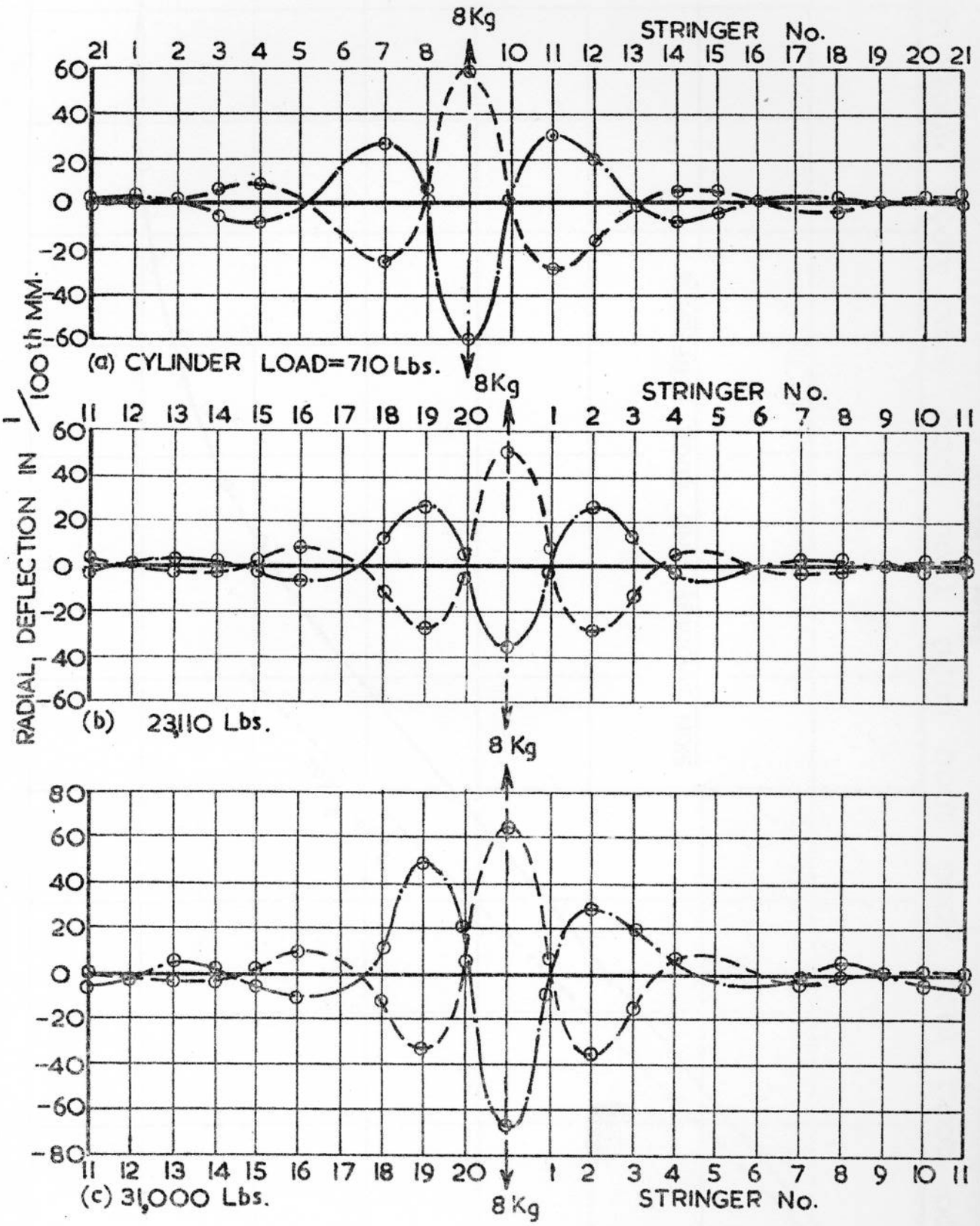

DEFLECTION OF FRAME 'C' UNDER ± 8 Kg PERTURBATION LOADS.

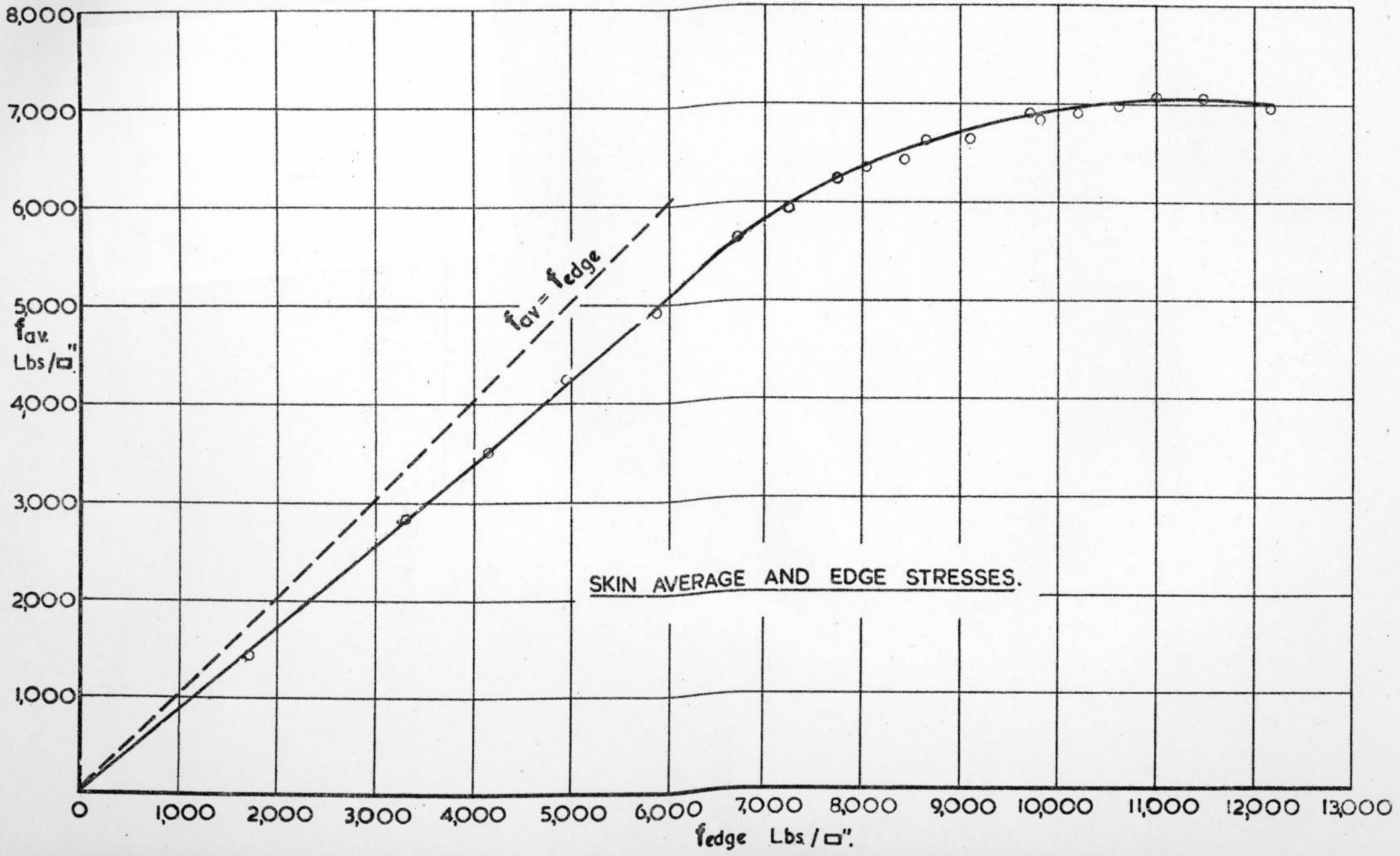
8,000
7,000
6,000
5,000
4,000
3,000
2,000
1,000
0
f_{av} Lbs/□".
$f_{av} = f_{edge}$
SKIN AVERAGE AND EDGE STRESSES.
1,000
2,000
3,000
4,000
5,000
6,000
7,000
8,000
9,000
10,000
11,000
12,000
13,000
f_{edge} Lbs/□".

FIG. 18.